Fluorine··· and π···Alkali Metal Interactions Control in the Stereoselective Amide Enolate Alkylation with Fluorinated Oxazolidines (Fox) as a Chiral Auxiliary: An Experimental and Theoretical Study

Gjergji Sini,*[a] Arnaud Tessier,[b] Julien Pytkowicz,[b] and Thierry Brigaud*[b]

Abstract: The α-alkylation of amide enolates by using a pseudo-C_2 symmetry *trans* 4-phenyl-2-trifluoromethyloxazolidine (*trans*-**Fox**) as a chiral auxiliary occurs with an extremely high diastereoselectivity (>99% de). The origin of this excellent stereocontrol was investigated by an experimental and theoretical (DFT) study. With this *trans* chiral auxiliary, both F···metal and π···metal interactions compete to give the same diastereomer through *Re* face alkylation of the enolate. A 5.5 kcal mol^{-1} energy difference found between the *Re* face and the *Si* face attack transition states is consistent with the complete diastereoselectivity that has been experimentally achieved.

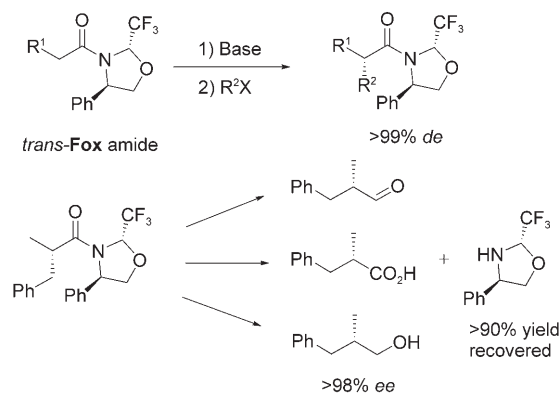On the other hand, in the case of the *cis* chiral auxiliary (*cis*-**Fox**) the competition between the F···metal and π···metal interactions is unfavourable to the diastereoselectivity. In this case, the *Re* face and the *Si* face attack transition states were found to be nearly isoenergetic (0.3 kcal mol^{-1} difference), which is in good agreement with the very low diastereoselectivity observed.

Keywords: alkali metals · asymmetric synthesis · density functional calculations · fluorine · transition states

Introduction

Owing to the specific properties of the fluorine atom, organofluorine compounds are finding an increasing interest mainly in the area of pharmaceuticals, agrochemicals and material sciences.[1] For these developments, the discovery of new chiral fluorine-containing synthons plays a crucial role.[2] During the ten last years, fluoral-based trifluoromethylated chiral oxazolidines (**Fox**) have emerged as powerful building blocks for the stereoselective synthesis of various chiral trifluoromethyl amino compounds.[3] In addition, we recently reported their use as high-performance chiral auxiliaries for the stereoselective alkylation of amide enolates.[4] The *trans* 4-phenyl-2-trifluoromethyloxazolidine (*trans*-**Fox**) proved to be an outstanding chiral auxiliary for the synthesis of enantiopure α-substituted aldehydes, carboxylic acids and β-substituted alcohols with a very efficient recovery of the chiral auxiliary (Scheme 1).

The use of fluorinated nitrogen heterocycles as chiral auxiliaries is mostly documented in the literature with highly fluorinated compounds for asymmetric fluorous catalysis,[5]

[a] Dr. G. Sini
Laboratoire LPPI, Université de Cergy-Pontoise
5 Mail Gay-Lussac, Neuville sur Oise
95031 Cergy-Pontoise cedex (France)
Fax: (+33) 134-257-071
E-mail: Gjergji.Sini@u-cergy.fr

[b] Dr. A. Tessier, Dr. J. Pytkowicz, Prof. Dr. T. Brigaud
Laboratoire "Synthèse Organique Sélective et Chimie Organométallique" (SOSCO), UMR CNRS 8123
Université de Cergy-Pontoise, 5 Mail Gay-Lussac
Neuville sur Oise, 95031 Cergy-Pontoise cedex (France)
Fax: (+33) 134-257-071
E-mail: thierry.brigaud@u-cergy.fr

Supporting information for this article is available on the WWW under http://www.chemeurj.org/ or from the author.

Scheme 1. Synthetic applications of *trans* 4-phenyl-2-trifluoromethyloxazolidine (*trans*-**Fox**) chiral auxiliary.

but the fluorine-containing group is rarely at the chiral centre. The use of fluorinated oxazolidinones with a per-fluoroalkyl chain[6] or a difluorobenzyl group[7] as chiral auxiliaries was recently reported. In the first case, the role of the perfluoroalkyl group is mainly to facilitate the chiral auxiliary recovery and in both cases the stereoselectivity does not seem to be oriented by interactions between the fluorine atoms and metals.

Fluorine···metal interactions, in a larger sense, have already been reported in the literature.[8] As they have been frequently evocated to explain specific reactivity and unusual diastereoselectivities of reactions involving metal containing fluorinated compounds,[9] we suspected the crucial role of such interactions to explain the extremely high diastereoselectivity of our reaction. To our knowledge, this would be the first application of the fluorine···metal interaction control with a fluorinated chiral auxiliary in asymmetric synthesis.
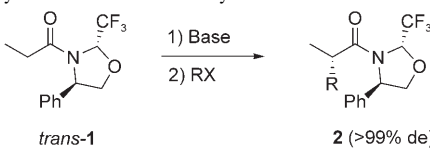
The study of the origin of the π-facial diastereoselection in enolate alkylation reactions is a current topic in organic synthesis. Its rationalization has been approached in the literature by both experimental and theoretical studies.[10] Therefore, with our chiral fluorinated oxazolidines (**Fox**) in hand, we carried out a theoretical study to gain more insight into the origin of the extremely high diastereoselectivity of the corresponding amide enolates alkylation.

Results and Discussion

Synthesis: The same high level of diastereoselectivity was achieved with Li, K and Na enolates (Table 1, entries 1–3).

The alkylation of *trans*-**1** was completely diastereoselective with benzyl bromide and with ethyl iodide (entry 4). Therefore the calculations were done with the less complex ethyl iodide. Moreover, we showed that the diastereoselectivity was not affected by the nature of the solvent. The same excellent reactivity and diastereoselectivity was achieved in different solvents such as THF and toluene (entries 3–5). However the benzylation reaction failed in hexane because of the very low solubility of the enolate in this non polar solvent. Moreover, the addition of 1,3-dimethyltetrahydro-2-pyrimidinone (DMPU) or *N,N,N′,N′*-tetramethylethylenediamine (TMEDA) may be expected to min-

Table 1. Diastereoselective alkylation reactions of *N*-acyl oxazolidine *trans*-**1**.


trans-**1**   2 (>99% de)

Entry	Base	Solvent	RX	Product Yield [%][a]	Ref
1	LiHMDS[b]	THF	BnBr	(S)-**2a** (82)	[c]
2	KHMDS	THF	BnBr	(S)-**2a** (63)	[c]
3	NaHMDS	THF	BnBr	(S)-**2a** (85)	[c]
4	NaHMDS	THF[d,e]	EtI	(S)-**2b** (78)	[c,f]
5	NaHMDS	toluene	BnBr	(S)-**2a** (58)	[f]
6	NaHMDS	THF/DMPU[g]	BnBr	(S)-**2a** (77)	[f]
7	NaHMDS	THF/TMEDA[h]	BnBr	(S)-**2a** (90)	[f]
8	LiHMDS	THF/TMEDA[i]	BnBr	(S)-**2a** (87)	[f]

[a] Yield of isolated product. [b] HMDS: hexamethyldisilazane. [c] Ref. [4]; [d] The reaction in toluene gave (S)-**2b** as a single diastereomer. [e] No reaction occurred in hexane. [f] This study. [g] THF/DMPU: 4:1. [h] THF/TMEDA: 4:1. [i] THF/TMEDA: 3:2.

Abstract in French: *L'auxiliaire chiral fluoré de pseudosymétrie* C$_2$ *trans-**Fox** (4-phenyl-2-trifluoromethyloxazolidine) permet l'α-alkylation des énolates d'amides avec une diastéréosélectivité exceptionnellement haute (> 99 % de). L'origine de cet excellent stéréocontrôle a été étudiée de façon expérimentale et théorique (DFT). Avec l'auxiliaire chiral trans-**Fox**, des interactions F···métal et π···métal sont en compétition mais conduisent au même diastéréoisomère via l'alkylation de l'énolate par la face Re. Une différence d'énergie de 5,5 kcal mol⁻¹ entre les états de transitions correspondant à l'attaque face Re et à l'attaque face Si est cohérente avec la totale diastéréosélectivité observée expérimentalement. Par contre, avec l'auxiliaire chiral de configuration cis (cis-**Fox**), la compétition entre les interactions F···métal et π···métal est néfaste à la diastéréosélectivité. Dans ce cas, la différence d'énergie entre les états de transitions correspondant aux attaques face Re et face Si est très faible (0,3 kcal mol⁻¹) expliquant la très faible diastéréosélectivité expérimentalement observée.*

imise coordination of the alkali metal with electron rich groups such as the enolate, the fluorine atoms or the phenyl group and to cause a decrease of the diastereoselectivity. In fact, intriguingly, this made no change and the diastereoselectivity remained unaffected (entries 6–8). This suggests that the geometry of the alkylation transition structures involves strong molecular interactions, which are not disturbed by the nature of the solvent.

As we have previously reported,[4] the benzylation of the *cis*-**1** oxazolidine amide enolate occurred with a very low diastereoselectivity (Scheme 2). In order to have an experimental reference for the theoretical study, the alkylation re-

R= Bn **3a** (55%, 69:31 *dr*)
R= Et **3b** (45%, 56:44 *dr*)
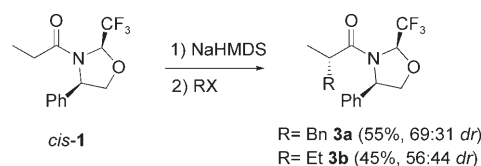
Scheme 2. Diastereoselective alkylation reactions of *N*-acyl oxazolidine *cis*-**1**.

action of *cis*-**1** was repeated with ethyl iodide. This reaction also proceeded with a very poor diastereoselectivity (Scheme 2). The theoretical study of this reaction was also carried out, to give an explanation of this low diastereoselectivity and to understand the differences with the *trans*-**1** case.

The contrasting results obtained from the *trans*-**Fox** and the *cis*-**Fox** chiral auxiliaries are apparently related to the *trans* or *cis* relative configurations of the CF₃ and the phenyl group. Each of them can play a double role: a steric one and a metal-attractive one. The steric role of the phenyl group is well known and largely used to explain stereoselective and chemoselective effects. Moreover, numerous experimental and theoretical studies provide evidence for the presence in many chemical structures of cation···π interactions of alkali metals with arenes.[11,9a] Most of them underline the presence of this type of interactions in the gas phase and solid-state structures, as well as in biological systems. To our knowledge, their implication in transition-state structures has never been clearly demonstrated. On the other hand, the trifluoromethyl group has been rarely used in the design of chiral auxiliaries. Although the steric hindrance of the trifluoromethyl group is well known,[12] CF₃···alkali metal interactions have been rarely reported. Only a few theoretical studies show that metal···F close contacts are able to provide rigidification of reaction intermediates and to stabilize specific transition states.[9a,h] Consequently, it could be suspected that Na···F and Na···π(Ph) interactions and their potential competition played a central role in our reactions. To our knowledge, these interactions have not yet been exploited in the chiral auxiliary strategy for the synthesis of enantiopure compounds.

In the following theoretical study we examine the exact role of the trifluoromethyl and the phenyl groups and we propose an explanation of their contribution to the diastereoselectivity of the reaction using the *trans*- and the *cis*-**Fox** chiral auxiliaries. To shed light on these questions, density functional calculations (DFT) were carried out by using GAUSSIAN98 program[13] at B3LYP/6-311+G(2d,p)// B3LYP/6-31G* level followed by polarisable conductor continuum model calculations (CPCM)[14] for the solvent effect (see computational details for further information).

***Trans*-Fox DFT study**: The *trans*-**1** sodium enolates, some of the weakly bonded enolate···ethyl iodide reactant complexes (**RC**) formed during the ethyl iodide approach together with the corresponding transition states (**TS**) were calculated and are shown in Figure 1. The ethylation of the *trans*-**1** enolate giving **2b** is discussed first. As it is commonly assumed for amide enolates, the first step of this reaction is the deprotonation of *trans*-**1** to give the resulting *Z* enolates in order to minimize the A-1;3 interactions.[15] Among the different possible enolates, the *trans*-**E1** and *trans*-**E2** structures (Figure 1) are the most stable, the latter is only 0.9 kcal mol⁻¹ higher in energy. *Trans*-**E1** presents an F···Na interaction with the sodium on the *Re* face of the enolate and *trans*-**E2** presents a π···Na interaction with the sodium

on the same *Re* face. Another enolate (*trans*-**E3**) presenting an F···Na interaction with the sodium on the *Si* face of the enolate is 1.9 kcal mol⁻¹ higher in energy. The geometrical parameters of *trans*-**E1** and *trans*-**E2** and the strongly positive Na charges clearly suggest strong electrostatic type Na···CF₃ and Na···π(Ph) interactions.[16] It could be concluded at this stage that the two interactions appear to be of comparable strength. These two interactions force the *trans*-**E1** and the *trans*-**E2** enolate plane to preferentially adopt a nearly coplanar position with respect to the oxazolidine mean plane. Considering for example the *trans*-**E1** case (Figure 1), it is clear that the presence of the sodium atom close to the *Re* face of the enolate will subsequently orientate the ethyl iodide approach by the same face through I···Na interaction giving rise to the weakly bonded complex *trans*-**RC1** (Figure 1).

This last complex is stabilized by both the Na···I interaction and a hydrogen type interaction between ethyl iodide and the enolate π-system. The role of the Na···CF₃ interaction seems to be twofold: rigidifying the structure of the enolate and orientating the ethyl iodide approach. The same could be said for the Na···π(Ph) interaction in the case of the *trans*-**E2** enolate.

To compare different reaction profiles three possible transition structures were located: *trans*-**TS1** (F···Na interaction, *Re* face attack), *trans*-**TS2** (π···Na interaction, *Re* face attack) and *trans*-**TS3** (F···Na interaction, *Si* face attack) (Figure 1).[17] The *trans*-**TS1** and *trans*-**TS2** structures corresponding to the *Re*-face alkylation of the enolate give the same (*S*)-**2b** product (Figure 1). The results show that *trans*-**TS2** is 2.4 kcal mol⁻¹ higher than *trans*-**TS1**, hence only the reaction profiles including *trans*-**TS1** and *trans*-**TS3** will be compared hereafter.

The reaction free energy profiles corresponding to the ethylation of the *Re* or the *Si* enolate faces giving (*S*)-**2b** or (*R*)-**2b** are shown in Figure 2.[18]

An energy comparison between the *trans*-TS1 and the *trans*-TS3 transition states shows that the *trans*-TS1 is the most stable one by 5.5 kcal mol⁻¹, which is in very good agreement with the high diastereoselectivity experimentally observed for this reaction (>99% de).[19] This result is also coherent with the simple idea that the best direction for the SN₂ attack in these reactions corresponds to the enolate face on which the sodium atom is located. On the other hand, the *trans*-TS2 transition structure presenting a π···Na interaction is 2.4 kcal mol⁻¹ higher in energy than *trans*-TS1. Consequently, it should be supposed that the reaction pathway giving rise to *trans*-TS2 also contributes to the result of the reactions. Fortunately, this small energy difference has no consequence on the stereochemical issue of the reaction. Actually, because of the pseudo-*C₂* symmetry of the *trans*-**Fox** chiral auxiliary, both transition states give the same (*S*)-**2b** product. It can be concluded at this stage that the alkali metal···F and the alkali metal···π(Ph) close contacts give rise to competitive transition states so both interactions should be considered to explain the diastereoselectivity of the reactions.
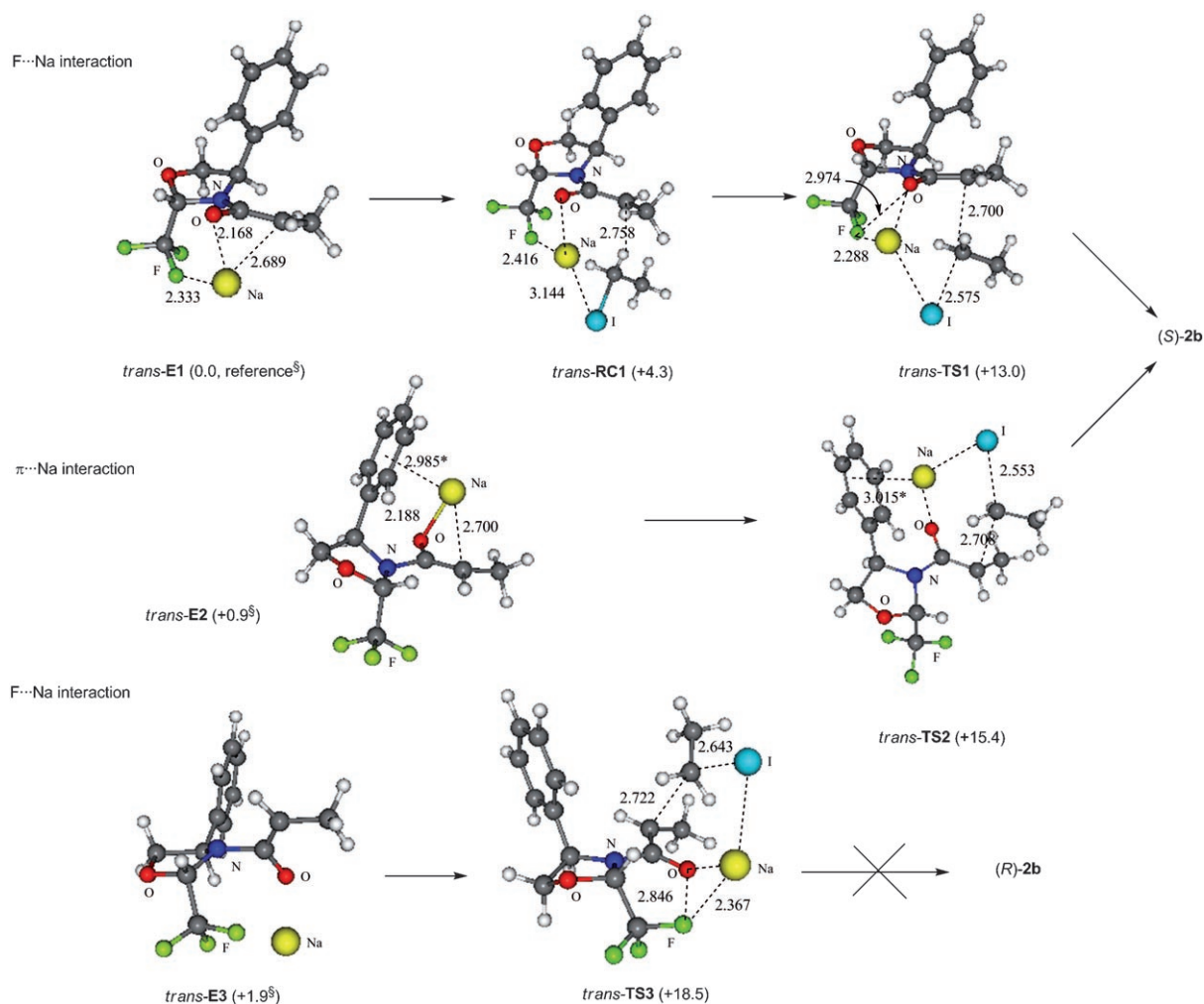
Figure 1. Optimised structures for *trans*-**1** enolates ethylation. Distances are given in Å (*=mean value for Na···Ph). The relative free energies [kcal mol⁻¹] are given in parentheses (§=also contains the energy of the isolated C₂H₅I species).
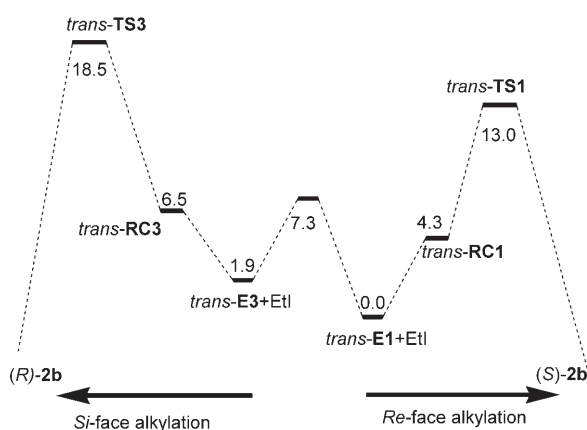

Figure 2. Relative free energies [kcal mol⁻¹] corresponding to the ethylation reaction of enolates *trans*-**E1** (*Re*-face alkylation) and *trans*-**E3** (*Si* face-alkylation).

***Cis*-Fox DFT study**: This last conclusion furnishes an explanation of the very low diastereoselectivity achieved in the *cis*-**1** enolate alkylation (Scheme 2). Actually, as in the

trans case, three transition states noted *cis*-**TS1**, *cis*-**TS2** and *cis*-**TS3** were calculated. The *cis*-**TS1** transition state is 4.7 kcal mol⁻¹ higher in energy than the others, so only *cis*-**TS2** and *cis*-**TS3** should be considered for the explanation of the poor diastereoselectivity of the reaction. The *cis*-**TS2** transition state is stabilised by a Na···π(Ph) interaction and corresponds to the *Re*-face ethylation (Figure 3), whereas
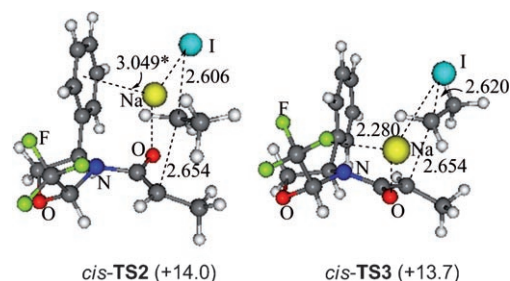

Figure 3. Optimised transition structures for the *cis*-**1** enolates ethylation. Distances are given in Å (*mean value for Na···Ph distance). The relative free energies [kcal mol⁻¹] are given in parentheses.

cis-**TS3** is stabilised by a Na···CF$_3$ interaction and corresponds to the *Si*-face alkylation (Figure 3).

   The key result is that *cis*-**TS2** and *cis*-**TS3** are nearly isoenergetic, the latter being only 0.3 kcal mol^{-1} lower in energy (Figure 4). In other words, the transition states based
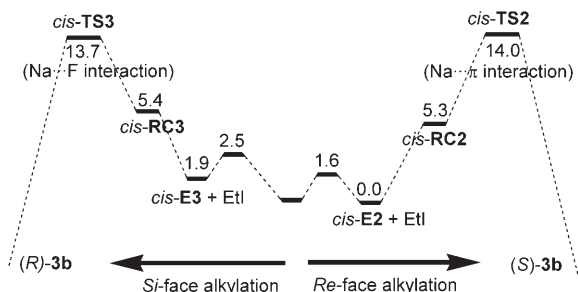

Figure 4. Relative free energies [kcal mol^{-1}] corresponding to the ethylation reaction of *cis*-**1**.

on Na···CF$_3$ and Na···π(Ph) interactions and giving rise to (*R*)-**2b** and (*S*)-**2b** products respectively, are in competition. A mixture of *R* and *S* products is therefore suggested by the calculations, which is in good agreement with the nearly equimolar diastereomeric mixture obtained experimentally.

Steric and electronic factors: It is worth highlighting at this point that despite the EtI···Ph proximity the *cis*-**TS3** transition state is found to be 1.2 kcal mol^{-1} lower than the *trans*-**TS1**. From a sterical point of view, one should expect that *trans*-**TS1** would be more stable (Figure 5), suggesting, in turn, that the steric hindrance of the phenyl group is not a determining factor for these reactions.
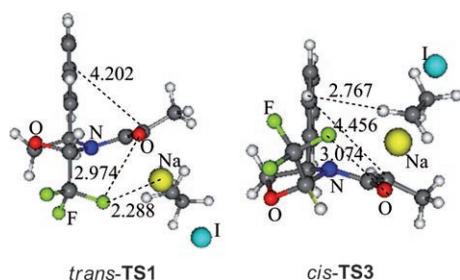

Figure 5. Comparison of *trans*-**TS1** and *cis*-**TS3**. Distances are given in Å.

   To evaluate the contribution of the π coordination of the phenyl group in the diastereoselectivity, the enolate alkylation reaction was experimentally performed with *trans*-**4** and *cis*-**4** valinol-based trifluoromethylated oxazolidines (Scheme 3).[20] Replacing the phenyl group by an isopropyl group caused a decrease in the diastereoselectivity. This result suggests that the electronic properties of the phenyl group are playing an important role in the control of the diastereoselectivity. Moreover, the steric effects associated
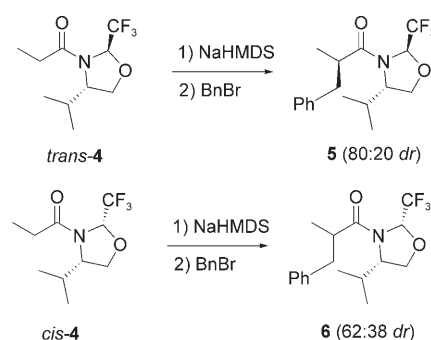
Scheme 3. Alkylation reactions of valinol-based *N*-acyl oxazolidines *trans*-**4** and *cis*-**4**.

to the isopropyl group do not provide a positive contribution to the diastereoselectivity.

   The contribution of the trifluoromethyl group was also estimated theoretically[21] in the case of a *trans*-oxazolidine chiral auxiliary having a methyl group in place of the trifluoromethyl one. The transition states corresponding to the *Re*-face and *Si*-face attacks are in this case separated by 2.9 kcal mol^{-1} in favour of the *Re*-face attack (see Figure 2 in the Supporting Information for the corresponding structures). Compared to the 5.5 kcal mol^{-1} calculated for the *trans*-**Fox** chiral auxiliary, this result suggests the important role of the trifluoromethyl group in the control of the diastereoselectivity.

Conclusion

Regrouping now the results of the alkylation reactions using the *trans*- and the *cis*-**Fox** chiral auxiliaries we can say that, as expected, the Na···CF$_3$ and Na···π(Ph) interactions play a central role in these reactions: rigidifying the reactant geometries and orientating the ethyl iodide approach leading to the corresponding precursor complexes and transition states. Moreover, the disappointing experimental results obtained with the valinol-based **Fox** and the theoretical results calculated with an unfluorinated oxazolidine suggest that both the CF$_3$ and the phenyl groups participate to achieve a good diastereoselectivity. It follows that the relative structural position between the trifluoromethyl and the phenyl groups becomes crucial for the diastereoselective control of these reactions. Two metal attractor groups disposed in a pseudo-C_2 symmetry (*trans*-**Fox**) give rise to the same product with a complete diastereoselectivity. On the other hand, when the chiral auxiliary presents two badly disposed metal attractor sites (pseudo-C_{2v} symmetry), the diastereoselective control of these reactions is ruined by competitive interactions. Based on these conclusions, we are currently investigating the design of novel fluorinated chiral auxiliaries.

Experimental Section

General information: Commercial reagents were purchased from Aldrich, Acros or Avocado and used as received. Trifluoroacetaldehyde-ethylhemiacetal was generously offered by Central Glass Company. All alkylation reactions were performed under argon atmosphere with oven-dried glassware fitted with rubber septa. Ether and THF were distilled under nitrogen from sodium/benzophenone prior to use. Flash chromatography was performed by using SDS 60A, (40–63 μm.) silica gel. Thin layer chromatography was performed on precoated aluminium sheets (MACHEREY-NAGEL ALUGRAM SIL/G 0.2 mm). They were visualized under a 254 nm UV light. ^{1}H NMR, ^{19}F NMR and ^{13}C NMR spectra were recorded by using a JEOL ECX-400 (^{1}H: 400 MHz; ^{19}F: 376.2 MHz; ^{13}C: 100.5 MHz). Chemical shift values (δ) are reported in ppm downfield from Me_4Si ($\delta = 0.0$ ppm), C_6F_6 ($\delta = -164.9$ ppm) or $CDCl_3$ as internal standard ($\delta = 77.0$ ppm). Data are reported as follows: chemical shift ($\delta = $ ppm), multiplicity (s = singlet, d = doublet, t = triplet, m = multiplet), integration, coupling constant (Hz). GC and low resolution mass spectra were performed by means of a Hewlett Packard GC 6890 coupled with a Hewlett Packard MSD 5973 apparatus (capillary column HP-5 MS, 30 m × 250 μm, He as vector gas, method: 70°C during 2 min, 20°C/min climb rate and 250°C during 15 min).

Experimental procedures: Experimental procedures and analytical data for oxazolidines *trans*-**1**, (*S*)-**2a**, (*S*)-**2b**, *cis*-**1** and **3a** were reported in our previous communication.[4]

Procedure for the benzylation reaction of *trans*-1 in toluene: The oxazolidine *trans*-**1** (0.321 g, 1.19 mmol) was dissolved in toluene (10 mL) under argon atmosphere. The solution was cooled down to −78°C and NaHMDS was added dropwise (1.12 mL, 2 M in THF, 2.24 mmol). The reaction mixture was stirred for 1.5 h at this temperature and the benzylbromide (0.269 mL, 2.24 mmol) was added slowly. The reaction mixture was stirred for 2 additional hours at −78°C, quenched with a saturated NH_4Cl solution (15 mL) and extracted with dichloromethane (2x30 mL). The combined organic layers were dried over $MgSO_4$, evaporated under reduced pressure and the resulting crude mixture was purified by filtration through a short pad of silica gel (cyclohexane/ethyl acetate: 90/10). (*S*)-**2a** (0.247 g, 58%) was obtained as a single diastereomer. No traces of the (*R*)-**2a** epimer were detected by GC. Spectral data of (*S*)-**2a** were identical to those reported in our preceding report.[4]

In a similar manner, the benzylation of the sodium enolate of *trans*-**1** (0.325 g, 1.19 mmol) in a THF/DMPU (10:1 mL) gave **2a** (0.332 g, 77%) as a single diastereomer. The benzylation of the sodium enolate of *trans*-**1** (0.325 g, 1.19 mmol) in a THF/TMEDA (8:2 mL) mixture gave **2a** (0.389 g, 90%) as a single diastereomer. The benzylation of the lithium enolate of *trans*-**1** (0.325 g, 1.19 mmol) in a THF/TMEDA (6:4 mL) mixture gave **2a** (0.375 g, 87%) as a single diastereomer. In any case, no traces of the (*R*)-**2a** epimer were detected by GC of the corresponding crude mixtures.

(2*R*,4*R*)-2-Trifluoromethyl-3-(-2-methylbutanoyl)-4-phenyloxazolidines (3b): To a solution of amide *cis*-**1** (0.360 g, 1.32 mmol) in THF (10 mL) under argon atmosphere at −78°C was added dropwise a solution of NaHMDS (1.25 mL, 2 M in THF, 2.5 mmol). The reaction mixture was stirred for 2 h at −78°C and ethyl iodide (0.2 mL, 2.5 mmol) was added. The reaction mixture was stirred for 3 additional hours at −78°C and the reaction mixture was quenched with a saturated NH_4Cl solution (15 mL) extracted with diethyl ether (2 × 30 mL) and dichloromethane (30 mL). The combined organic layers were dried over $MgSO_4$, evaporated under reduced pressure and the resulting crude mixture was purified by filtration through a short pad of silica gel (cyclohexane/ethyl acetate, 90:10). **3b** (0.178 g, 45%) was isolated as a 56:44 mixture of diastereomers and a fraction of unreacted starting material *cis*-**1** (0.145 g, 36%) was recovered.

3b (major diastereomer): GC: $R_t = 9.52$ min; ^{1}H NMR (250 MHz, CDCl$_3$): $\delta = 0.88$ (t, 3H, $^3J = 7.4$ Hz), 1.09 (d, 3H, $^3J = 6.7$ Hz), 1.26–1.68 (m, 2H), 2.31 (m, 1H), 4.11 (m, 1H), 4.62 (m, 1H), 5.09 (m, 1H), 6.02 (m, 1H), 7.18–7.39 ppm (m, 5H); ^{19}F NMR (235.35 MHz, CDCl$_3$): $\delta = $ −77.84 ppm (m, 3 F); MS: *m/z* (%): 301 (M$^+$, 52), 273 (5), 217 (15), 203 (27), 188 (56), 148 (36), 120 (31), 104 (24), 85 (51), 57 (100).

3b (minor diastereomer): GC: $R_t = 9.47$ min; ^{1}H NMR (250 MHz, CDCl$_3$): $\delta = 0.52$ (m, 3H), 0.88 (t, 3 H, $^3J = 7.4$ Hz), 1.26–1.68 (m, 2H), 2.31 (m, 1H), 4.11 (m, 1H), 4.62 (m, 1H), 5.09 (m, 1H), 6.02 (m, 1H), 7.18–7.39 ppm (m, 5H); ^{19}F NMR (235.35 MHz, CDCl$_3$): $\delta = $ −77.63 ppm (d, 3 F, $^3J_{H-F} = 5.4$ Hz); MS: *m/z* (%): 301 (M$^+$, 52), 273 (4), 217 (14), 203 (27), 188 (56), 148 (35), 120 (29), 104 (22), 85 (49), 57 (100).

Computational methods: The calculations in this study were carried out at the DFT (B3LYP) and MP2 theory levels, using the GAUSSIAN98 program.[13] During the geometry optimisations the internal 6-31G* basis set was used for all the atoms except iodine for which the Lanl2DZ ECP and valence shell basis set was chosen[22a–c] augmented by one polarization function ($\zeta = 0.289$).[22d,e] The same basis set for I atom was used afterwards for higher level energy comparisons. To estimate the error induced by this last limitation, test calculations were done at B3LYP/aug-cc-pvdz//B3LYP/6-31G* level which resulted with a change of the energy difference by only 0.2 kcal mol^{-1} (the aug-cc-pvdz-pp basis for I and aug-cc-pvdz basis for Na were chosen from reference 22f).

Geometries: Different conformations were considered for the oxazolidine cycle (with H at the N atom instead of an acyle group) containing the phenyl and CF_3 groups in trans and cis positions. The most stable conformers were used afterwards as starting geometries during the optimisations of enolates, reactant complexes and the transition states. All the geometry optimisations were followed by frequency calculations showing no imaginary frequencies for the minimum structures and only one imaginary frequency for the transition state structures. Further analysis of the vibrational modes associated to the imaginary frequencies showed correspondence between the transition state structures and the reactants (products).

Solvent effect: The influence of the solvent on the reactions (THF in this case) was considered by carrying out single point energy calculations in the frame of CPCM continuum model.[14] The PCM continuum model[23] was also tested but the results shown in the Table 2 and discussed here-

Table 2. Energy differences [kcal mol^{-1}] between some representative transition states.[a] $a = 6$-311 + G(2d,p)//B3LYP/6-31G* [b] the experimental result in this case is indirectly deduced. The "0" value is based on the fact that a mixture of 56% (*S*) and 44% (*R*) products was obtained. See the text hereafter for more details.

	PCM		CPCM		
	B3LYP/a[a]	MP2/a[a]	B3LYP/a[a]	MP2/a[a]	Exp[b]
$\Delta E_{trans\text{-}TS3-trans\text{-}TS1}$	4.3	7.1	5.5	7.7	–
$\Delta E_{trans\text{-}TS2-trans\text{-}TS1}$	1.6	0.1	2.4	−0.1	–
$\Delta E_{cis\text{-}TS2-cis\text{-}TS3}$	−2.0	−2.4	0.3	−1.4	"0"

after suggest that the CPCM model gives in this case better agreement with experimental result. The effect of CPCM calculations on the energy differences between transition states is less than 1 kcal mol^{-1} which seems coherent with the small dipole moments of these species. These results are also in line with the identical experimental results obtained with the same reactions carried out in solvents of different polarity (THF and toluene).[24]

B3LYP versus MP2 methods: Different studies have shown that DFT methods in general, and B3LYP in particular, fail in determining some thermochemistry parameters such as reaction enthalpies so MP2/6-31 + G* or MP2/6-31 + G*//B3LYP/6-31 + G* level studies are recommended.[25a,b] It has also been shown that B3LYP fails to describe the M···π interactions, although it does well in the case of electrostatic M^{+n}···π interactions.[25c] To test the reliability of our model chemistry we carried out some test calculations at B3LYP/6-311 + G(2d,p)//B3LYP/6–1G* and MP2/6-311 + G(2d,p)//B3LYP/6-31G* levels. The energy differences between some representative reactants and transition states are shown in Table 2.

The nature of these species is described in the paper and it is not important to detail here. It could be simply said that *trans*-**TS2** and *cis*-**TS2** species involve Na···π(Ph) interactions while the others contain Na···F interactions. The results in the table indicate non negligible changes between B3LYP versus MP2 methods. As it is shown in the paper these differences do not affect the chemical interpretations and the agreement with the experimental results. However, these differences remain important for discussing the competing physical phenomena inside these structures (comparison between Na···π(Ph) and Na···F interactions). As DFT and MP2 methods are known to respectively underestimate and overestimate the electronic correlation experimental values were necessary for comparison. In the absence of other experimental thermochemistry parameters, we considered that the mixture of 56 % (*S*) versus 44 % (*R*) products obtained in the case of *cis*-**1** giving **3** reactions (Scheme 2) could serve as a good indication for comparing the corresponding transition states. Actually, in the case of this reaction only two transition states were found to be in competition, each presenting only one competing conformational isomer (other isomers differing on the oxazolidine cycle conformation were found to be roughly 3 kcal mol^{-1} higher in energy). Therefore, in view of the experimental result an energy difference of roughly 0 kcal mol^{-1} could be supposed to be found between the two competing transition states (*cis*-**TS3** and *cis*-**TS2** in this case). The results (Table 1, third line) show that CPCM/B3LYP and CPCM/MP2 approaches describe this reaction correctly. Both results seem to be different by less than 1 kcal mol^{-1} roughly from the supposed experimental value of 0 kcal mol^{-1}, with the (*S*)/(*R*) ratio being slightly underestimated by the B3LYP result and slightly overestimated by the MP2 one. For the sake of smaller computational cost the B3LYP/6-311+G(2d,p)//B3LYP/6-31G* approach was then adopted.

Energies: The energy values given in the paper and used for the discussions correspond to the free energies obtained at CPCM/B3LYP/6-311+G(2d,p)//B3LYP/6-31G* level. The corrections for the free energies are taken at the experimental temperature (195.15 K) and are scaled by a factor of 0.9804 to take into account the systematic errors in the frequency values.

However, it has been evocated[26] that ΔS^{+} values contain errors, owing to the low frequency intermolecular vibrational modes and the neglect of their anharmonic character. The energy differences between equivalent species (between transition states or between enolates) vary by less than 1 kcal mol^{-1}, owing to the entropic effects, meaning that the agreement with the experimental results is not affected. On the other hand, the activation free energy values (ΔG^{+} with respect to the reactants) are approximately 8 kcal mol^{-1} greater than the corresponding ΔH^{+}. The ΔG^{+} values could consequently contain errors, which we can not estimate owing to a lack of experimental thermochemistry parameters.

Despite this, we prefer presenting the free energy values because of the more realistic shape of the reaction profiles. Although the entropy problem does not modify the comparison between the competing transition states and the corresponding conclusions, one should be prudent with the absolute values of the activation parameters given in the Figure 2 and Figure 4.

Finally, the basis set superposition error (BSSE) was calculated for all the transition state structures and the reactant complexes by the counterpoise approach.[27] The BSSE values were found to vary between 1.1–1.2 kcal mol^{-1} and are included in the relative energy values presented here.

Acknowledgements

[1] a) R. D. Chambers, *Fluorine in organic chemistry*, Oxford, Blackwell Boca Raton, CRC Press, **2004**; b) T. Hiyama, *Organofluorine Compounds, Chemistry and applications*, (Ed: H. Yamamoto), Springer-Verlag, Berlin Heidelberg, **2000**; c) P. Kirsch, *Modern fluoroorganic chemistry: synthesis, reactivity, applications*, Wiley-VCH, Weinheim, **2004**; d) *Organofluorine Chemistry, Principles and Commercial Applications*, (Eds R. E. Banks, B. E. Smart, J. C. Tatlow), Plenum: New York, **1994**.

[2] a) *Fluorine-containing synthons*, (Ed. V. A. Soloshonok), American Chemical Society, Washington, DC, **2005**; b) *Enantiocontrolled Synthesis of Fluoro-Organic Compounds*, (Ed. V. A. Soloshonok), Wiley, Chichester, UK, **1999**; c) *Asymmetric Fluoroorganic Chemistry: Synthesis, Applications, and Future Directions*, (Ed. P. V. Ramachandran), ACS Symp. Ser. No. 746, American Chemical Society, Washington, DC, **2000**; d) *Organofluorine Chemistry* (Ed. K. Uneyama), Blackwell, **2006**.

[3] a) A. Ishii, K. Higashiyama, K. Mikami, *Synlett* **1997**, 1381–1382; b) N. Lebouvier, C. Laroche, F. Huguenot, T. Brigaud, *Tetrahedron Lett.* **2002**, *43*, 2827–2830; c) F. Gosselin, A. Roy, P. D. O'Shea, C. Cheng, R. P. Volante, *Org. Lett.* **2004**, *6*, 641–644; d) W. C. Black, C. I. Bayly, D. E. Davis, S. Desmarais, J.-P. Falgueyret, S. Leger, C. S. Li, F. Massé, D. J. McKay, J. T. Palmer, M. D. Percival, J. Robichaud, N. Tsou, R. Zamboni, *Bioorg. Med. Chem. Lett.* **2005**, *15*, 4741–4744; e) T. Billard, B. R. Langlois, *J. Org. Chem.* **2002**, *67*, 997–1000; f) J. Legros, F. Meyer, M. Coliboeuf, B. Crousse, D. Bonnet-Delpon, J.-P Bégué, *J. Org. Chem.* **2003**, *68*, 6444–6446; g) F. Huguenot, T. Brigaud, *J. Org. Chem.* **2006**, *71*, 2159–2162; h) F. Huguenot, T. Brigaud, *J. Org. Chem.* **2006**, *71*, 7075–7078.

[4] A. Tessier, J. Pytkowicz, T. Brigaud, *Angew. Chem.* **2006**, *118*, 3759–3763; *Angew. Chem. Int. Ed.* **2006**, *45*, 3677–3681.

[5] F. Fache, *New J. Chem.* **2004**, *28*, 1277–1283.

[6] a) J. E. Hein, P. G. Hultin, *Synlett* **2003**, 635–638; b) J. E. Hein, J. Zimmerman, M. P. Sibi, P. G. Hultin, *Org. Lett.* **2005**, *7*, 2755–2758; c) J. E. Hein, P. G. Hultin, *Tetrahedron: Asymmetry* **2005**, *16*, 2341–2347.

[7] Santos Fustero, J. Piera, J. F. Sanz-Cervera, P. Bello, N. Mateu, *J. Fluorine Chem.* **2007**, *128*, 647–653.

[8] a) H. Takemura, S. Nakashima, N. Kon, M. Yasutake, T. Shinmyozu, T. Inazu, *J. Am. Chem. Soc.* **2001**, *123*, 9293–9298; b) B. Goldfuss, P. V. R. Schleyer, S. Handschuh, F. Hampel, *J. Organomet. Chem.* **1998**, *552*, 285–292; c) H. Plenio, *Chem. Rev.* **1997**, *97*, 3363–3384; d) H. Plenio, *ChemBioChem*, **2004**, *5*, 650–655; e) ref[1b] pp. 129–135; f) ref[2a] pp. 399–411; g) ref[2d] pp. 139–172.

[9] a) N. J. R. van Eikema Hommes, P. von R. Schleyer, *Angew. Chem.* **1992**, *104*, 768–771; *Angew. Chem. Int. Ed. Engl.* **1992**, *31*, 755–758; b) Y. Morizawa, A. Yasuda, K. Uchida, *Tetrahedron Lett.* **1986**, *27*, 1833–1836; c) T. Hanamoto, T. Fuchikami, *J. Org. Chem.* **1990**, *55*, 4969–4971; d) N. Shinohara, J. Haga, T. Yamazaki, T. Kitazume, S. Nakamura, *J. Org. Chem.* **1995**, *60*, 4363–4374; e) T. Yamazaki, M. Ando, T. Kitazume, M. Kubota, M. Omura, *Org. Lett.* **1999**, *1*, 905–908; f) K. Tamura, T. Yamazaki, T. Kitazume, T. Kubota, *J. Fluorine Chem.* **2005**, *126*, 918–930; g) H. Ito, A. Saito, T. Taguchi, *Tetrahedron: Asymmetry* **1998**, *9*, 1989–1994; h) Y. Itoh, M. Yamanaka, K. Mikami, *J. Am. Chem. Soc.* **2004**, *126*, 13174–13175; i) M. Shimizu, T. Fujimoto, H. Minezaki, T. Hata, T. Hiyama, *J. Am. Chem. Soc.* **2001**, *123*, 6947–6948; j) M. Shimizu, T. Fujimoto, L. Xinyu, H. Minezaki, T. Hata, T. Hiyama, *Tetrahedron* **2003**, *59*, 9811–9823; k) T. Ritter, M. W. Day, R. H. Grubbs, *J. Am. Chem. Soc.*, **2006**, *128*, 11768–11769.

[10] a) K. Ando, N. S. Green; Y. Li, K. N. Houk, *J. Am. Chem. Soc.* **1999**, *121*, 5334–5335; Y. Li, K. N. Houk, *J. Am. Chem. Soc.* **1999**, *121*, 5334–5335; b) K. Ando, *J. Am. Chem. Soc.* **2005**, *127*, 3964–3972; c) Y. Itkuta, S. Tomoda, *Org. Lett.* **2004**, *6*, 189–192; d) A. I. Meyers, M. A. Seefeld, B. A. Lefker, J. F. Blake, P. G. Williard, *J. Am. Chem. Soc.* **1998**, *120*, 7429–7438; e) C. Aydillo, G. Jiménez-Osés, J. H. Busto, J. M. Peregrina, María M. Zurbano, A. Avenoza, *Chem. Eur. J.* **2007**, *13*, 4840–4848; f) G. Jiménez-Osés, C. Aydillo, J. H. Busto, M. M. Zurbano, J. M. Peregrina, A. Avenoza, *J. Org.*

Chem. **2007**, *72*, 5399–5402; g) I. Soteras, O. Lozano, A. Gómez-Esqué, C. Escolano, M. Orozco, M. Amat, J. Bosch, F. J. Luque, *J. Am. Chem. Soc.* **2006**, *128*, 6581–6588; h) S. D. Bull, S. G. Davies, M.-S. Key, R. L. Nicholson, E. D. Savory, *Chem. Commun.* **2000**, 1721–1722; i) S. D. Bull, S. G. Davies, A. C. Garner, D. Kruchinin, M.-S. Key, P. M. Roberts, E. D. Savory, A. D. Smith, J. E. Thomson, *Org. Biomol. Chem.* **2006**, *4*, 2945–2964; j) S. D. Bull, S. G. Davies, A. C. Garner, A. L. Parkes, P. M. Roberts, T. G. R. Sellers, A. D. Smith, J. A. Tamayo, J. E. Thomson, R. J. Vickers, *New J. Chem.* **2007**, *31*, 486–495; k) J. Mulzer, O. Langer, M. Hiersemann, J. W. Bats, J. Buschmann, P. Luger, *J. Org. Chem.* **2000**, *65*, 6540–6546; l) F. Andersson, E. Hedenström, Tetrahedron: Asymmetry **2006**, *17*, 1952–1957.

[11] a) J. Sunner, K. Nishizawa, P. Kebarle, *J. Phys.Chem* **1981**, *85*, 1814–1820; b) D. A. Dougherty, *Science*, **1996**, *271*, 163–168; c) J. Wouters, *Protein Sci.* **1998**, *7*, 2472–2475; d) S. L. De Wall, L. J. Barbour, G. W. Gokel, *J. Am. Chem. Soc.* **1999**, *121*, 8405–8406; e) V. Ryzhov, R. C. Dunbar, *J. Am. Chem. Soc.* **1999**, *121*, 2259–2268; f) R. C. Dunbar, *J. Phys. Chem. A* **2002**, *106*, 7328–7337; g) J. Sivaguru, R. B. Sunoj, T. Wada, Y. Origane, Y. Inoue, V. Ramamurthy, *J. Org. Chem.* **2004**, *69*, 6533–6547.

[12] a) M. Schlosser, D. Michel, *Tetrahedron* **1996**, *52*, 99–108; b) D. O'Hagan, H. S. Rzepa, *Chem. Commun.* **1997**, 645–652.

[13] Gaussian 98 (Revision A.7), M. J. Frisch, G. W. Trucks, H. B. Schlegel, G. E. Scuseria, M. A. Robb, J. R. Cheeseman, V. G. Zakrzewski, J. A. Montgomery, Jr., R. E. Stratmann, J. C. Burant, S. Dapprich, J. M. Millam, A. D. Daniels, K. N. Kudin, M. C. Strain, O. Farkas, J. Tomasi, V. Barone, M. Cossi, R. Cammi, B. Mennucci, C. Pomelli, C. Adamo, S. Clifford, J. Ochterski, G. A. Petersson, P. Y. Ayala, Q. Cui, K. Morokuma, D. K. Malick, A. D. Rabuck, K. Raghavachari, J. B. Foresman, J. Cioslowski, J. V. Ortiz, B. B. Stefanov, G. Liu, A. Liashenko, P. Piskorz, I. Komaromi, R. Gomperts, R. L. Martin, D. J. Fox, T. Keith, M. A. Al-Laham, C. Y. Peng, A. Nanayakkara, C. Gonzalez, M. Challacombe, P. M. W. Gill, B. G. Johnson, W. Chen, M. W. Wong, J. L. Andres, M. Head-Gordon, E. S. Replogle, J. A. Pople, Gaussian, Inc., Pittsburgh, PA, **1998**.

[14] V. Barone, M. Cossi, *J. Phys. Chem. A* **1998**, *102*, 1995–2001.

[15] D. Evans, J. M. Takacs, *Tetrahedron Lett.* **1980**, *21*, 4233–4236.

[16] The NPA charge on Na atom for *trans*-**E1** structure is 0.90. ELF calculations and total electronic density surfaces on this structure (Figure 1, Supporting Information) confirm the nearly pure electrostatic nature of the Na···F interaction. For more details about ELF method see; B. Silvi, A. Sevin, *Nature* **1994**, *371*, 683–686.

[17] The common characteristic of the three transition states is that the I···C distances are 16–21% longer than in the reactants, while the C···C distances are approximately 78% longer than the C-C distance in the final product (*S*)-**2b**. These transition states are consequently much closer to the reactants than to the products and can be considered as early type transition states.

[18] The calculated $\Delta S^{\neq}$ values contain errors owing to the low frequency intermolecular vibrational modes and the neglect of their anharmonic character. Although this problem does not modify the comparison between the competing transition states and the corresponding conclusions, one should be prudent with the absolute values of the activation parameters given in the Figures 2 and 4. (for more information see computational details)

[19] Different observations could help to understand this energy difference but it seems to be mainly controlled by the following: the *trans*-**TS3** structure shows that ethyl iodide approaches the enolate face opposite to the CF₃ group. This *trans*-**TS3** transition state suffers then from a weaker Na···F attractive interaction than *trans*-**TS1** ($d_{Na···F} = 2.367$ Å for *trans*-**TS3** versus 2.288 Å for *trans*-**TS1**, Figure 1) and a stronger repulsive F···O$_{enolate}$ interaction ($d_{F···O} = 2.846$ Å versus 2.974 Å respectively, Figure 1). Moreover, to optimise the F···O$_{enolate}$ and F···Na interactions the CF₃ group in *trans*-**TS3** adopts a nearly eclipsed conformation with respect to the oxazolidine cycle (the dihedral F-C-C-O$_{cycle}$ angle is $-24.1°$) as compared to the unstrained stagered conformation for *trans*-**TS1** (the F-C-C-O$_{cycle}$ angle is $-60.9°$). We point out that this nearly eclipsed conformation is absent in *trans*-**E3** enolate. This unfavourable situation for *trans*-**TS3** seems to be reinforced by the Et-I···Ph proximity. As a conclusion, the *trans*-**TS1** structure takes advantage of all these electronic and steric factors.

[20] *trans*-**4** and *cis*-**4** were obtained by our standard acylation procedure[4] from the CF₃-oxazolidines prepared from (*S*)-valinol and trifluoroacetaldehyde methyl hemiacetal.[3]

[21] Because of the hydrolytical instability of the chiral auxiliary, this reaction could not be performed experimentally.

[22] a) P. J. Hay, W. R. Wadt, *J. Chem. Phys.* **1985**, *82*, 270–283; b) idem page 284–298; c) idem, page 299–310; d) A. Höllwarth, M. Böhme, S. Dapprich, A. W. Ehlers, A. Gobbi, V. Jonas, K. F. Köhler, R. Stegmann, A. Veldkamp, G. Frenking, *Chem. Phys. Lett.* **1993**, *208*, 237–240; e) A. W. Ehlers, M. Böhme, S. Dapprich, A. Gobbi, A. Höllwarth, V. Jonas, K. F. Köhler, R. Stegmann, A. Veldkamp, G. Frenking, *Chem. Phys. Lett.* **1993**, *208*, 111–114; f) K. A. Peterson, D. Figgen, E. Goll, H. Stoll, M. Dolg, *J. Chem. Phys.* **2003**, *119*, 11113–11123.

[23] a) S. Miertus, J. Tomasi, *Chem. Phys.* **1981**, *55*, 117–129; b) S. Miertus, J. Tomasi, *Chem. Phys.* **1982**, *65*, 239–245; c) M. Cossi, V. Barone, R. Cammi, J. Tomasi, *Chem. Phys. Lett.* **1996**, *255*, 327–335.

[24] a) the dielectric constant values for these two solvents could seem not very different ($\varepsilon = 7.58$ for THF as compared to $\varepsilon = 2.379$ for toluene). However, it has been shown (references b and c hereafter) that the change in the solvent effect is very rapid for small dielectric constants. The difference in polarity between THF and toluene could consequently bee sufficient for testing the solvent effect in these reactions. b) G. Sini, M. Bellassoued, N. Brodie, *Tetrahedron* **2000**, *56*, 1207–1215; c) B. Bogdanov, T. B. McMahon, *Int. J. Mass Spectrom.* **2005**, *241*, 205–223.

[25] a) C. E. Check, T. M. Gilbert, *J. Org. Chem.* **2005**, *70*, 9828–9834; b) L. M. Pratt, N. V. Nguyên, B. Ramachandran, *J. Org. Chem.* **2005**, *70*, 4279–4283; c) C. Aleman, D. Curco, J. Casanovas, *Phys. Rev. E* **2005**, *72*, 026704.

[26] a) A. A. Mohamed, F. Jensen, *J. Phys. Chem. A* **2001**, *105*, 3259–3268; b) B. Bogdanov, T. B. McMahon, *Int. J. Mass Spectrom.* **2005**, *241*, 205–223.

[27] S. F. Boys, F. Bernardi, *Mol. Phys.* **1970**, *19*, 553–566.